Pulse Arrival Scheduling for Nanonetworks under Limited IoT Access Bandwidth

Hang Yu, Bryan Ng, Winston K.G. Seah
School of Engineering and Computer Science
Victoria University of Wellington, Wellington, New Zealand
Email: { hang.yu, bryan.ng, winston.seah }@ecs.vuw.ac.nz

***Abstract*—Electromagnetic Wireless Nano Sensor Networks (EM-WNSNs) with molecule-level sensing capacity benefit a wide range of applications that demand high resolution. To accommodate the potentially high data volume, small antenna size, and limited energy capacity, the high-speed TeraHertz (THz) pulses sparsely distributed over time are adopted for communications among nano devices. For EM-WNSNs connected to the Internet of Things (IoT), matching the throughput of nanonetworks and the IoT access bandwidth is significant for resource utilization efficiency. On the one hand, high throughput from nano sensors are limited by IoT access bandwidth, which results in low energy efficiency of EM-WNSNs when traffic regulation mechanisms are applied. On the other hand, low throughput from nanonetworks under utilize the allocated access bandwidth. To enable efficient data forwarding towards the access network, the EM-WNSNs throughput must match the IoT access bandwidth. For this purpose, the Adaptive Pulse Interval Scheduling (APIS) scheme, which schedules the arrival pattern of pulses transmitted by nano sinks based on the access bandwidth, is proposed for event-based EM-WNSNs. From performance evaluation and modelling, APIS implements data forwarding with high energy efficiency for nanonetworks and high bandwidth efficiency for IoT access networks. To the best of our knowledge, APIS is the first pulse-level access scheduling solution for EM-WNSNs connected to the IoT.**

I. Introduction

The fast development of nano technology is envisaged to realize the Electro-Magnetic Wireless Nano Sensor Networks (EM-WNSNs) that have ultra-high sensing capacity. To date, a substantial amount of research on individual components such as nano sensors [1], nano antennas [2], nano transceivers [3], nano energy harvester [4], and nano actuator [5] has been conducted. With the nano-scale resolution, deep insights could be obtained for applications that demand microscopic observations with fast response. Besides improving the accuracy of traditional micro-scale applications, the non-invasive feature of nanonetworks also enable emerging applications such as software-defined materials [6], micro robotics [7], and in-vivo sensing [8].

Considering the small-sized antenna and the limited energy capacity, information exchanged among nano devices is carried by 100-fs-long pulses in the TeraHertz (THz) band (0.1 THz - 10 THz). Due to the wide bandwidth of THz band, the theoretical transmission speed of one point-to-point link is up to Tbps, which can provide unprecedented high aggregated throughput from the network [9]. Nevertheless, when EM-WNSNs are connected to the Internet of Things (IoT), high throughput without awareness of potential bottleneck at the access network may reduce the resource utilization efficiency.

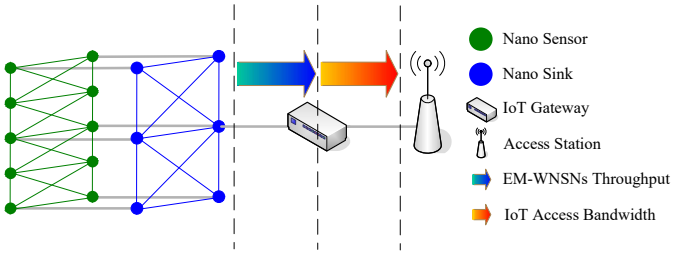

Fig. 1: Nanonetworks connected to the Internet

For EM-WNSNs connected to IoT, the direction of data flow is shown in Fig 1. The sensed data of nano sensors are first aggregated at nano sinks and then forwarded to the gateway. Next, the gateway transmits the data to the access network via access points or base stations. Unfortunately, the current access technologies for Machine-Type Communications (MTC) such as LoRa [10], LTE-MTC [11], and NB-IoT [12] are designed for low-bandwidth access; thus, they cannot accommodate the high throughput of EM-WNSNs especially with bursty transmissions [13].

When the mismatch between EM-WNSNs throughput and IoT access bandwidth happens, the resource utilization efficiency of both nanonetworks and access networks may be compromised. On the one hand, for the EM-WNSNs throughput that exceed the access bandwidth, traffic policing mechanisms drop data or traffic shaping mechanisms buffer data and this leads to either unnecessary energy consumption for nano devices or the demand for large buffer at IoT gateways. On the other hand, consistently reducing EM-WNSNs throughput not only affects information quality [14] but also underutilizes the access bandwidth allocated.

To achieve high resource utilization efficiency of the overall network, the throughput of nanonetworks should match the access bandwidth. For this purpose, the Adaptive Pulse Interval Scheduling (APIS) is proposed for event-based EM-WNSNs under limited access bandwidth. When bursty events occur, APIS adjusts the EM-WNSNs throughput by scheduling the pulse positions and intervals of nano sinks based on the allocated access bandwidth. As a result, the data from EM-WNSNs could be forwarded by the IoT gateway without being buffered or dropped, which eliminates the need for

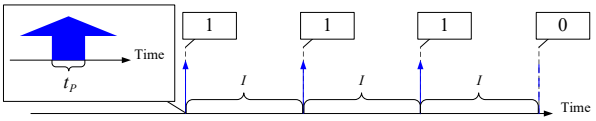

Fig. 2: TS-OOK modulation

retransmissions. Performance evaluation and modelling show that APIS achieves high energy efficiency for nanonetworks and high bandwidth efficiency for access networks.

Our contributions in this paper are:

1) We propose a lightweight pulse arrival scheduling method, namely APIS, for event-based nanonetworks under limited IoT access bandwidth. APIS is the first pulse-level accessing solution that enables efficient bridging from nano-scale communications to the overall IoT.
2) We develop mathematical models of bandwidth efficiency and unit energy consumption for the proposed APIS scheme. Those models provide accurate performance guidelines for different network configurations.

The rest of the paper is organized as follows. In section II, the background knowledge of the pulse-based modulation scheme and the related work on data acquisition in EM-WNSNs are reviewed. The design details of APIS are presented in Section III, followed by performance evaluation and modelling in Section IV and V, respectively. Finally, the conclusions are shown in Section VI.

II. Background and Related Work

In this section, we first review the background knowledge including pulse-based modulation for EM-WNSNs and the existing backhaul techniques for IoT. Next, the related work on data collection schemes for EM-WNSNs is discussed.

A. Pulse modulation for EM-WNSNs

To exchange information among nano devices deployed in the aforementioned scenarios, the Time Spread On-Off Keying (TS-OOK) [15], is adopted. TS-OOK modulation utilizes 100-fs-long THz pulses with long pulse intervals to modulate the signal to be communicated. Specifically, as shown in Fig. 2, the appearance and absence of pulses are used to modulate bit 1 and 0, respectively. The raw throughput C_R of a single communication link, which could be up to Tbps [9] because of the wide bandwidth of THz band, is given by Eqn. (1) [16]:

$$C_R = \frac{1}{t_P + I}, \tag{1}$$

where t_P denotes the pulse duration with a value of 100 fs for THz pulses and I is the pulse interval.

TS-OOK not only accommodates the small antenna size but also achieves high communication efficiency in two aspects. First, with pulses sparsely distributed over time, high aggregated network throughput becomes feasible via interleaved transmissions of multiple sources [17]. Second, energy consumption, co-channel interference, and collision probability are minimized by means of low-weight coding schemes [18].

B. Data collection for EM-WNSNs

For densely deployed nano devices that are networked for sensing tasks, data collection schemes play a significant role in achieving high communication efficiency that is vital for resource-constrained nodes. Related research work regarding data collection could be classified into two categories: sender-initiated schemes and receiver-initiated schemes.

Sender-initiated schemes are suitable for event-driven and time-driven applications [19]. The first sender-initiated data collection scheme is a cross-layer design composed of a routing framework [20] and a MAC protocol [17] which target perpetual network operations. When a nano sensor is ready to transmit data for event reporting, it communicates with the corresponding nano sink to request the MAC scheduling and routing decision that are scheduled considering energy efficiency. As a result, the nano sensor will transmit the data with the tuned transmission power and the allocated time slots.

Extracting data from in-vivo scenarios faces the challenge of dynamic channel conditions. For nanonetworks monitoring human lungs, molecular absorption varies due to the inhalation and exhalation of oxygen and carbon dioxide, resulting in dynamic path loss and noise level. For data acquisition with low energy consumption in this scenario, an algorithm [8] utilizing the periodic window exhibiting low molecular absorption is proposed to optimize the energy efficiency.

Receiver-initiated data collection schemes are designed for query-based applications [19]. To implement efficient data collection under dynamic THz channel conditions and limited access bandwidth, a protocol stack composed of the On-demand Efficient polling (OE polling) [21] and the TTL-based Efficient Forwarding (TEForward) [22] are proposed. In OE polling, based on the latest access bandwidth, the IoT gateway tunes the packet aggregation size of nano sinks by inserting a special field into the polling beacon. In response, nano sinks receiving the beacon aggregate the corresponding number of packets from nano sensors. Next, the data aggregated is sent using TEForward which provides nano devices with a lightweight forwarding solution under dynamic topology.

The cooperative Raman Spectroscopy [23] provides an architecture to collect data for in-vivo sensing. In this system, data collection is started by a network of on-body nano sensors emitting optical signals with the optimized power allocation for different sub bands. In-vivo sensors that are exposed to the propagated signals would be excited to scatter a spectrum band which contains the molecular information of the sensing area. Lastly, the scattered spectrum is detected and reconstructed by the on-body sensors via centralized or distributed Raman spectrum estimation algorithm.

Most of the existing work deals with stand-alone nanonetworks without considering the limited IoT access bandwidth. Although OE polling captures this constraint, the query-based data collection limits the application scenario. To fill the gap, APIS is proposed for event-driven EM-WNSNs under limited access bandwidth.

III. Proposed solution

In this section, the ideal pulse arrival pattern at the EM-WNSN gateway and the design of APIS are discussed.

A. Ideal pulse arrival

For EM-WNSNs connected to the Internet, matching the EM-WNSNs throughput to the available bandwidth of the access network is significant for the sake of resource utilization efficiency. Given the allocated access bandwidth B, the pulse duration t_P and pulse interval I, to achieve the maximal data rate without triggering traffic regulation mechanisms, we may relate I with B using Eqn. (2):

$$\frac{1}{t_P + I} = B, \tag{2}$$

which allows us to calculate the shortest pulse interval I_S that leads to the ideal arrival pattern of pulses which maximally utilizes the access bandwidth with on-demand throughput, as shown in Fig. 3. Thus, we have:

$$I_S = \frac{1}{B} - t_P. \tag{3}$$

Pulses arriving at the gateway that are not separated by intervals of duration I_S contribute to poor energy efficiency of nanonetworks and poor bandwidth utilization of access networks. On the one hand, for nano devices, unnecessary energy is consumed when pulses arrive densely with intervals shorter than I_S only to be dropped at the gateway (by traffic policing mechanisms). On the other hand, for IoT access networks, sparse pulses with intervals longer than I_S introduces bandwith efficiency. Based on the aforementioned observations, we devise a scheme that adapts the pulse interval to achieve both energy and bandwidth efficiency.

B. Overview of APIS

The APIS scheme uses a distributed algorithm run by nano sinks in small-scale single-hop EM-WNSNs detecting bursty events. The APIS algorithm adapts to access bandwidth and neighbour degree and schedules the pulses transmitted from nano sinks to the IoT gateway based on the ideal pulse arrival pattern. Since APIS operates on nano sinks, the process that aggregates data from nano sensors to nano sinks is highly abstracted in this work. The design of APIS is presented in Algorithm 1.

The APIS algorithm comprises two scheduling steps, which are the transmission shifting and interleaving. Both steps are based on the network information collected from short channel sensing. Specifically, when nano sinks start transmitting pulses when events happen, transmissions of nano sinks are first shifted in sequence with an interval of I_S. Next, multi-user transmissions are interleaved by separating pulses with the interval that evenly shares the bandwidth among nano sinks. Therefore, pulses arrive at the gateway in accordance with the ideal pattern. APIS only involves simple addition and multiplication operations with linear time complexity $\mathcal{O}(N')$ whereby N' denotes the actual number of sinks transmitting on event occurrence, therefore it is suitable for resource-constraint nano devices.

The APIS has the following operation assumptions:

1) Each nano sink is one-hop connected to other nano sinks and the IoT gateway.
2) Nano sinks are preconfigured with parameters I_S and the total number of nano sinks N. This can be easily achieved by the IoT gateway broadcasting a configuration beacon.
3) Nano sinks are in receiving mode for channel sensing when events occur. This is a feasible operation for nano sinks that are designed for data collection.
4) High time precision is required for scheduling. According to the existing research on nanonetworks [8], [24], [25], this is feasible for nano devices deployed in nano-scale scenarios with tiny propagation delay.

C. APIS preamble

For transmission detection, each original packet starts with an initialization preamble of a bit "1" [15]. In comparison, an APIS packet adopts a preamble containing "1" followed by "0" to present the first bit in each packet, as shown in Fig. 4. The "1" in the beginning, which carries the sequence information of multi-source transmissions, is only used for transmission shifting. Therefore, they are transmitted directly in a burst without shifting. The following "0" compensates the energy consumption of "1". When it reaches the time to receive "0", the IoT gateway inverses "0" to "1" and sends it to the access network as the first bit. In this way, transmission shifting is accomplished without losing the first bit under traffic policing. With the introduction of one extra bit, an APIS packet achieves the same energy consumption and introduces marginal delay compared with the original packet.

D. Transmission shifting

The transmission shifting aims to sequence the transmissions of individual nano sinks with an interval of I_S in alignment with the first sink transmitting. To reach this goal, for each sink except the first one, two local parameters are required. First, the transmission time of the global first pulse, t_1. Here, we define the global i-th pulse as the i-th pulse among pulses from all sinks whereas the local i-th pulse denotes the i-th pulse from one particular sink. Second, the number of neighbours that access the channel prior to the current sink, S.

Transmission shifting begins with the transmission of the global first pulse. After transmitting this pulse, the first sink shifts its subsequent transmission by a long interval I_L given in Eqn. (4):

$$I_L = NI_S. \tag{4}$$

I_L ensures sufficient time for preamble exchange considering the potential time spread of events and the computational latency of nano sinks, which is significant for successful scheduling. The gateway is also aware of I_L so as to detect the global first "0" and following "0"s in APIS preambles that

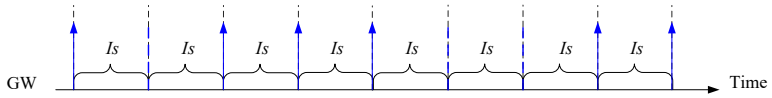

Fig. 3: Ideal pulse arrivals at the gateway

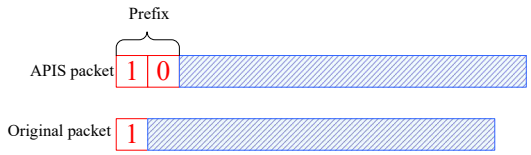

Fig. 4: Packet structure

Algorithm 1 Adaptive Pulse Interval Scheduling (APIS)

Transmitting mode

1: **if** reaches the time t_{TX}^{i} to transmit the i-th pulse **then**
2: Transmit the pulse
3: **if** $TxCount \leq 2$ **then**
4: $TxCount++$
5: **end if**
6: **if** $TxCount == 1$ **then**
7: **if** $S == 0$ **then**
8: $I = I_L$
9: **else**
10: $I = t_1 - t_{TX}^{1} + I_L + SI_S$
11: **end if**
12: **else if** $TxCount == 2$ **then**
13: $I = (ND+1)I_S + NDt_P$
14: Stop channel sensing
15: **end if**
16: Transmit the next pulse after I
17: **end if**

Receiving mode

1: **if** Receive the j-th pulse at time t_{RX}^{j} **then**
2: **if** $TxCount == 0$ **then**
3: **if** $j == 1$ **then**
4: $t_1 = t_{RX}^{1}$
5: **end if**
6: $S++$
7: **end if**
8: $ND++$
9: **end if**

are sequentially separated by I_S. The latency introduced by I_L is found to be marginal compared to the total transmission as discussed in section V.

For each sink receiving the global first pulse at time t_{RX}^{1}, t_1 is obtained by recording t_{RX}^{1}, as shown by step 4 in the receiving mode of Algorithm 1. Inferring the transmission time of the global first pulse from the receiving process is reliable for small-scale EM-WNSNs with short propagation delay. Next, as in step 6 in the receiving mode, S for each sink is obtained by counting the number of preamble "1"s received before transmitting the local first pulse, which is conditioned on $TxCount == 0$ whereby $TxCount$ is a two-bit long transmission counter.

After transmitting the preamble "1" at time T_{TX}^{1}, a nano sink will shift its subsequent pulses by an interval I given in step 10 in the transmitting mode of Algorithm 1. I is the sum of three parts, namely, I_L, $T_{RX}^{1} - T_{TX}^{1}$, and SI_S. The

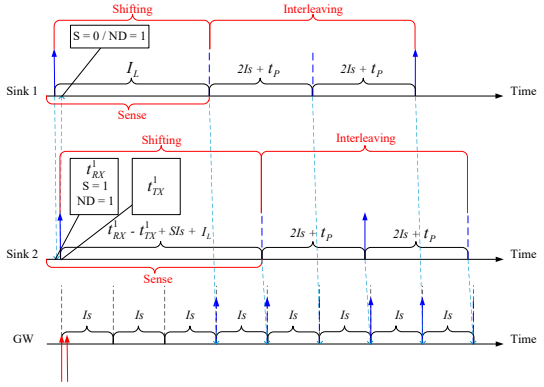

Fig. 5: Adaptive pulse interval Scheduling ($N' = 2, N = 3$)

subsequent transmission of the current sink will first be aligned to the first sink via $T_{RX}^{1} - T_{TX}^{1} + I_L$ and then shifted to be I_S later than the neighbour sink transmitting prior to it via SI_S.

E. Transmission interleaving

After shifting the transmissions of all nano sinks, subsequent pulses from all sinks following APIS preambles will be interleaved with an interval that evenly shares the bandwidth. Assuming there are N' out of N sinks active for transmission, the bandwidth allocated for each sink becomes $\frac{B}{N'}$. By replacing B with $\frac{B}{N'}$ in Eqn (2), the pulse interval I for subsequent pulses is derived in Eqn. (5):

$$I = \frac{N'}{B} - t_P = N'I_S + (N'-1)t_P. \tag{5}$$

The value of N' is obtained by counting the number of "1"s in APIS preambles received during the channel sensing, which implies the neighbour degree ND, as presented by step 8 in the receiving mode of Algorithm 1. Finally, by replacing N' with $ND+1$ in Eqn. (5), I is updated in step 13 in the transmitting mode of Algorithm 1. As shown in the following steps, each nano sink transmits subsequent pulses with the interval I and stops sensing the channel after the transmission time of the preamble "0" since sufficient information has been obtained.

F. APIS example

The full operations of APIS is depicted via the example in Fig. 5. Two out of three nano sinks, which are Sink 1 and Sink 2, are transmitting pulses to the IoT gateway. Sink 1 transmits the global first pulse and shifts its subsequent transmission by I_L. When Sink 2 receives this pulse at t_{RX}^{1}, it approximates t_1 with t_{RX}^{1} and increments both S and ND to 1 since Sink 1 transmits prior to it. After the transmitting the local first pulse at t_{TX}^{1}, Sink 2 shift its next transmission by $t_{RX}^{1} - t_{TX}^{1} + SI_S + I_L$. By receiving the local first pulse of Sink 2, Sink

1 only increments ND to 1 since Sink 2 transmits after it. When it reaches the time for the local second pulses, which are "0"s in preambles, the pulse interval of both Sink 1 and Sink 2 are set to $I = 2I_S + t_P$ which interleaves transmissions of two sinks with evenly shared bandwidth. Channel sensing is then stopped.

IV. Performance evaluation

This section first defines the performance metrics used for performance evaluation and lists several benchmark schemes for comparison, followed by the simulation parameters. At last, performance results are presented and analysed.

A. Performance metrics

1) Bandwidth efficiency, BE:

$$BE = \frac{\lambda_E}{B}, \tag{6}$$

where λ_E is the effective throughput that denotes the actual throughput after traffic policing.

2) Pulse drop ratio, D:

$$D = \frac{N^D_{pulse}}{N_{pulse}}, \tag{7}$$

where N^D_{pulse} is the number of pulses dropped by traffic policing at the gateway and N_{pulse} is the total number of pulses received by the gateway.

3) Fairness, F:

$$F = \frac{(\sum_{i=1}^{N'} \lambda_E^i)^2}{N' \sum_{i=1}^{N'} \lambda_E^i)^2}, \tag{8}$$

where λ_E^i is the effective throughput of the i-th sink.

4) Packet delivery ratio, PDR:

$$PDR = \frac{N^E_{pkt}}{N_{pkt}}, \tag{9}$$

where N^E_{pkt} is the number of packets effectively forwarded to the access network and N_{pkt} is the total number of packets from nanonetworks. The access network fails to receive a packet if any pulse in the packet is dropped.

5) Unit energy consumption, E:

$$E = \frac{E_{total}}{N^E_{pulse}}, \tag{10}$$

where E_{total} denotes the total energy consumption at nano sinks transmitting pulses and N^E_{pulse} is the number of pulses effectively forwarded to the access network after traffic policing.

B. Benchmarks

To benchmark the APIS, the following lightweight scheduling schemes are adopted. They investigate the effects of neighbour awareness (with/without the knowledge of neighbour degree) and multiple-user arrival pattern (sequential/interleaved) on pulse arrival scheduling.

1) Long Pulse Interval Scheduling (LPIS). In LPIS, pulses are transmitted directly with a fixed interval I_L.
2) Random Pulse Interval Scheduling (RPIS). RPIS is similar to LPIS but with random pulse intervals. For each pulse to be transmitted, the interval is given by a random number RI_S whereby $R \in [1, N]$.
3) Short Pulse Interval Scheduling (SPIS). SPIS originates from the basic unslotted Carrier-Sense Multiple Access with Collision Avoidance (CSMA/CA). Before transmitting the first pulse, the nano sink conducts channel sensing for I_S. All pulses are then transmitted with an interval of I_S if the channel is clear. Otherwise, an one-packet-long backoff time is adopted before the next channel sensing.
4) Short Pulse Interval Scheduling with Random Backoff (SPIS-RB). SPIS-RB is SPIS with random backoff time that is given by RI_S with $R \in [0, P_{size} - 1]$ where P_{size} denotes the packet size.

C. Simulation parameters

Performance of the pulse scheduling schemes is evaluated using the Nano-Sim package [26] on NS-3 with pulse-level simulations enabled. Simulation parameters are listed in Table I. The adopted scenario comprises 10 to 50 nano sinks randomly deployed following uniform distribution in a $10cm \times 10cm \times 10cm$ 3D space with the IoT gateway located at the geometric centre. To establish direct links among network devices, the following communication parameters are adopted. Each bit "1" is carried by a 100-fs-long pulse on 100 GHz with energy e_{TX} of 1 aJ and receiver sensitivity of -130 dBm based on the reported capacity of nano materials [21], [22]. The molecular absorption coefficient K [15] that determines THz channel conditions is set to 2.6e-5m^{-1} given by HITRAN (HIgh resolution TRANsmission) molecular absorption database ("USA Model, Mean Latitude, Summer, H=0") [27]. Each nano sink has a 50% probability to transmit for event reporting when events occur considering that nano devices are configured for heterogeneous sensing tasks in reality [28]. To simulate nano-scale bursty events, in each simulation, a nano sink starts transmitting one packet at a random starting time $t_{start} \in [0\mu s, 20\mu s]$. Each packet has a size P_{size} of 256 bits (257 bits for APIS) with a 50% probability of bit "1" [18]. The access bandwidth B is set to 200 Kbps following NB-IoT. Considering the low-cost feature of IoT devices, traffic policing activated every $\frac{1}{B}$ time with a precision of microseconds is deployed at the gateway. Simulation finishes when all nano sinks finish transmitting their pulses. The results are presented using mean values with 95% confidence intervals of 50 simulations. Each figure contains the full comparison and the magnified details of APIS at the bottom.

TABLE I: Simulation Parameters

Parameter	Value
Frequency	100 GHz
Pulse energy e_{TX}	1 aJ
Pulse duration t_P	100 fs
Receiving sensitivity	-130 dBm
Packet size P_{size}	256 bits (257 bits for APIS)
Event time t_{start}	[0 μs, 20 μs]
Simulation area	10 cm $\times$ 10 cm $\times$ 10 cm
Network size N	10 - 50 with a step of 5
IoT gateway position	Geometric centre
Nano sink position / mobility	Uniform / static
Molecular absorption coefficient K	2.6e-5 m^{-1}
Access bandwidth B	200 Kbps

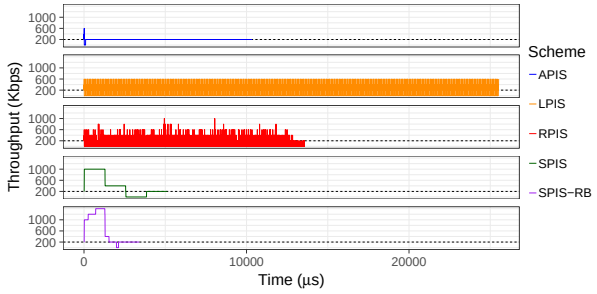

Fig. 6: Raw throughput over time ($N = 20$)

D. Results and analysis

To explore the pulse arrival pattern before traffic policing, one sample of raw throughput over time for a network with 20 sinks is shown in Fig. 6. As expected, APIS throughput mostly matches the access bandwidth of 200 Kbps except for the spike in the beginning due to the bursty "1"s in APIS preambles. In comparison, benchmark schemes mostly mismatch the access bandwidth. From the averaged bandwidth efficiency in Fig. 7, after traffic policing, APIS utilizes 99.61% of the bandwidth on average because of the find-grained arrival pattern. Below APIS, SPIS and SPIS-RB achieve 94.63% and 96.64% efficiency, respectively, benefiting from the short pulse interval adopted and the medium access mechanism that actively competes for transmission opportunities. Unfortunately, this high efficiency comes from the raw throughput that exceeds the bandwidth, which happens due to the wrong estimation of channel states when neighbours are transmitting "0"s that cannot be sensed. LPIS shows the lowest bandwidth efficiency due to two reasons. First, the interval I_L shares B among the total number of nano sinks rather than the ones transmitting, which underutilizes B. Second, simply confining transmission speed does not suffice to implement the ideal arrival pattern.

The pulse drop ratio is presented in Fig. 8. Under traffic policing, APIS only loses the first pulses in preambles, which is shown in Fig. 9 that depicts the ID distribution of the pulses dropped, so the pulse drop ratio is consistently 3.89% given by $\frac{N'}{N'P_{size}}$. In comparison, SPIS-based schemes exhibits high pulse drop ratio as a result of the fixed interval and the false channel estimation that jointly result in consecutive pulse dropping. RPIS achieves the second lowest pulse drop ratio

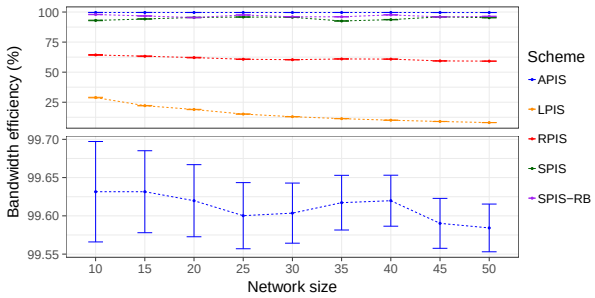

Fig. 7: Bandwidth efficiency vs network size

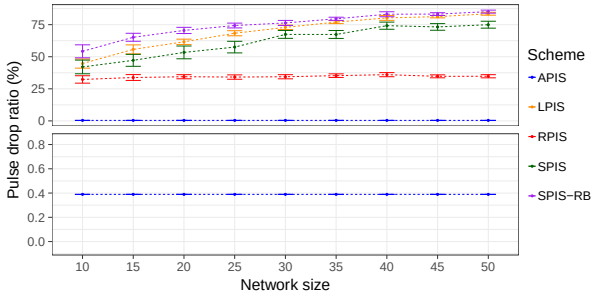

Fig. 8: Pulse drop ratio vs network size

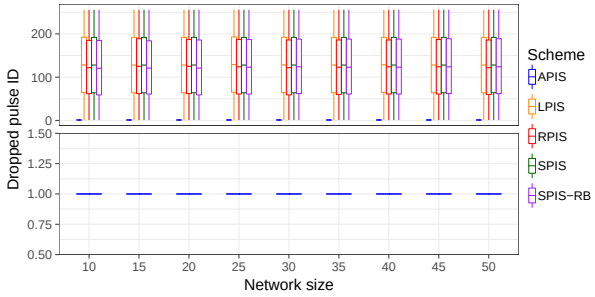

Fig. 9: Dropped pulse ID vs network size

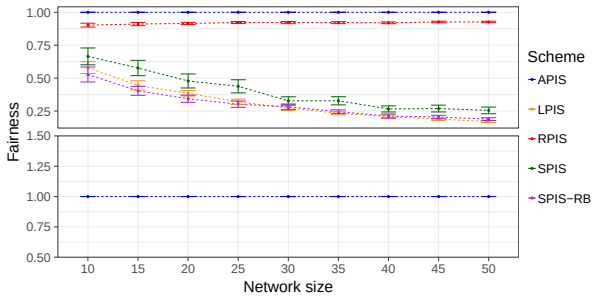

Fig. 10: Fairness vs network size

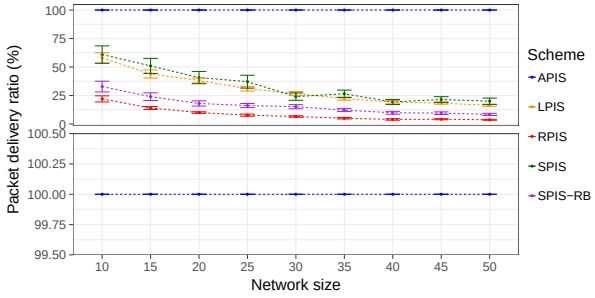

Fig. 11: Packet delivery ratio vs network size

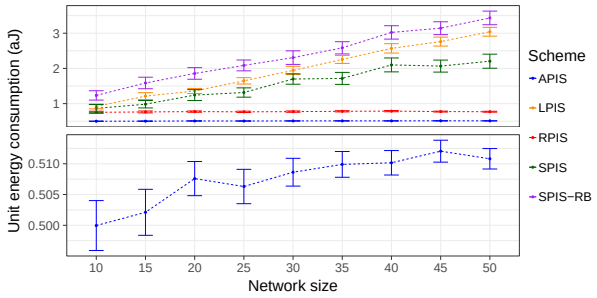

Fig. 12: Unit energy consumption vs network size

since the random arrival pattern reduces the probability of two pulses consistently arriving within I_S. Again, without shifting transmission, LPIS experiences high pulse drop ratio.

Pulse drop ratio is positively correlated with fairness shown in Fig. 10. This is because that when pulses from different senders arrive within I_S, only the pulse of the first sender is retained with others dropped. Because of the transmission interleaving that evenly shares bandwidth among nano sinks, APIS consistently shows a fairness index of 1.

Besides, discarding pulses leads to packet loss in the absence of retransmission and advanced error correction mechanisms. Fig. 11 shows that APIS achieves 100 % packet delivery ratio as a result of no pulse loss except the "1"s in preambles, which implies retransmission-free data delivery. This feature is significantly beneficial for nano devices with constrained energy capacity. Compared with APIS, packet loss is observed to all benchmark schemes. It is worth noticing that there is no direct relationship between pulse drop ratio and packet loss ratio since the latter is determined by the pulse loss distribution among packets.

As shown in Fig. 12, the high bandwidth efficiency and low pulse drop ratio of APIS benefit the energy efficiency. The unit energy consumption is close to the theoretically lowest level that is 0.5 aJ given that each packet contains 50% bit "1". However, the APIS preamble indeed gives rise to slightly more unit energy consumption due to the number of preambles "1"s received that increases quadratically with the network size. The high energy efficiency extends the network lifetime and relaxes the demand for energy providers when energy harvesting is applied on nano devices.

Overall, APIS provides a solution for connecting EM-WNSNs to the Internet through bandwidth-limited access networks. It presents both high energy efficiency for nanonetworks and high bandwidth efficiency for access networks.

V. Performance Modelling

In this section, the performance modelling of bandwidth efficiency and unit energy consumption are developed and validated to serve as a guideline for network configurations when APIS is applied.

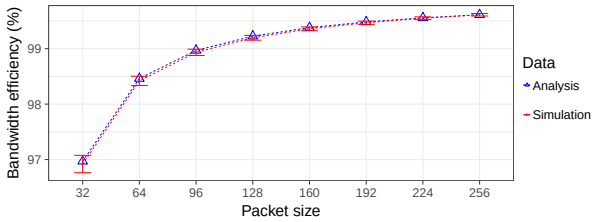

Fig. 13: Effective throughput modelling

A. Effective throughput

To obtain the bandwidth efficiency BE in Eqn. (6), the effective throughput λ_E is required. λ_E is given by

$$\lambda_E = \frac{N^E_{pulse}}{\tau}, \tag{11}$$

where τ is the total transmission time of nano sinks.

For APIS, since the first pulse in preamble is not retained, N^E_{pulse} can be obtained as

$$N^E_{pulse} = (P_{size} - 1)N', \tag{12}$$

By summing all pulse durations, the long waiting interval, and the total short pulse intervals in transmission, τ is calculated as

$$\tau = t_P P_{size} N' + I_L + I_S(P_{size} - 2)N', \tag{13}$$

with number of nano sinks transmitting is given by:

$$N' = \alpha N, \tag{14}$$

where α denotes the probability that one sink involves in pulse transmission. In this work, α is set to a constant of 0.5.

By substituting Eqn. (3), Eqn. (4), and Eqn. (11) - Eqn. (14) into Eqn. (6), BE is expressed as

$$BE = \frac{P_{size} - 1}{Bt_P P_{size} + (1 - Bt_P)(P_{size} - 2 + \frac{1}{\alpha})}. \tag{15}$$

It can be seen that BE is proportional to P_{size}, which is validated through simulations with various P_{size} from 33 to 257 with a step of 32, as shown in Fig. 13. This is because that a long packet size mitigates the effect of idle channel during the APIS prefix. Nano sinks that are normally configured with large packet sizes could efficiently utilize the access bandwidth with APIS.

B. Unit energy consumption

The total energy consumption of the nano sinks transmitting pulses E_{total}, which is required for obtaining E in Eqn. (10), is given as

$$E_{total} = E^{TX}_{total} + E^{RX}_{total}, \tag{16}$$

where E^{TX}_{total} and E^{RX}_{total} are the total energy consumption for transmitting and receiving, respectively.

Since one APIS packet contains the 2-bit APIS preamble that is"10" and the remaining $P_{size} - 2$ bits, E^{TX}_{total} can be expressed as

$$E^{TX}_{total} = e_{TX} N' \Big(\beta(P_{size} - 2) + 1\Big), \tag{17}$$

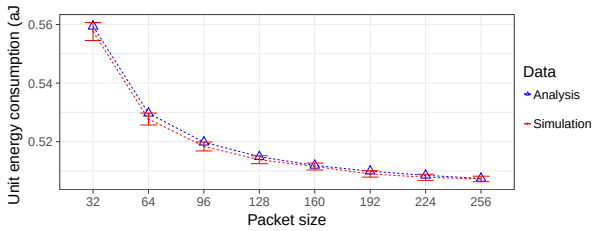

Fig. 14: Unit energy consumption vs packet size

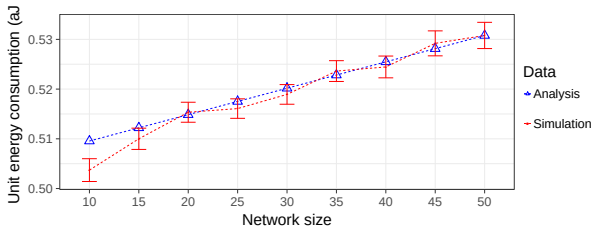

Fig. 15: Unit energy consumption vs network size

where β is the ratio of bit "1" to bit "0" that is set to 50% in this work.

For APIS, pulse receiving only happens during the sensing period before the transmission time of the second bit in one APIS preamble. Therefore, E_{total}^{RX} is given by

$$E_{total}^{RX} = e_{RX} N'(N' - 1), \tag{18}$$

where e_{RX} is the energy consumption for receiving one pulse.

Using the common assumption that the energy consumed for receiving one pulse is 10% of the amount consumed for transmitting one pulse [16], we have

$$e_{RX} = 0.1 e_{TX}. \tag{19}$$

Finally, by substituting Eqn. (12), Eqn. (14), and Eqn. (16) - Eqn. (19) into Eqn. (10), E can be expressed as

$$E = e_{TX}\left(\frac{\beta(P_{size} - 2) + 0.1\alpha N + 0.9}{P_{size} - 1}\right). \tag{20}$$

Based on the final model, packet size and total number of sinks are the influencing parameters for unit energy consumption. Therefore, the comparison between the analytical model and simulation results for various P_{size} and N are shown in Fig. 14 and Fig. 15, respectively. As discussed in section IV-D, unit energy consumption is impacted by the energy consumed by the APIS preamble. Therefore, increasing the P_{size} reduces the percentile of preamble in the total transmission, which decreases E. On the contrary, E increases with N since the number of preambles received increases quadratically with the network size.

VI. Conclusions

Nanonetworks connected to the overall IoT face the challenge of limited IoT access bandwidth. To achieve high resource utilization efficiency, a distributed lightweight pulse scheduling scheme, namely APIS, is proposed for event-based nanonetwork. Adopting simple operations with low complexity, APIS schedules pulses following the ideal arrival pattern when events happen. From performance evaluation and modeling, APIS, which is the first pulse-level accessing solution for nanonetworks, achieves high energy efficiency for nanonetworks and high bandwidth efficiency for IoT access networks.

VII. Acknowledgement

This research is supported by Victoria's Huawei NZ Research Programme, Software-Defined Green Internet of Things project (E2881) and Victoria Doctoral Scholarship.

References

[1] C. R. Yonzon, D. A. Stuart, X. Zhang, A. D. McFarland, C. L. Haynes, and R. P. V. Duyne, "Towards advanced chemical and biological nanosensorsan overview," *Talanta*, vol. 67, no. 3, pp. 438 – 448, 2005, nanoscience and Nanotechnology. [Online]. Available: http://www.sciencedirect.com/science/article/pii/S0039914005003504

[2] L. Zakrajsek, E. Einarsson, N. Thawdar, M. Medley, and J. M. Jornet, "Lithographically defined plasmonic graphene antennas for terahertz-band communication," *IEEE Antennas and Wireless Propagation Letters*, vol. 15, pp. 1553–1556, 2016.

[3] J. M. Jornet and I. F. Akyildiz, "Graphene-based plasmonic nano-transceiver for terahertz band communication," in *Antennas Propag. (EuCAP), 2014 8th Eur. Conf.* IEEE, 2014, pp. 492–496.

[4] Z. L. Wang, "Towards self-powered nanosystems: From nanogenerators to nanopiezotronics," *Advanced Functional Materials*, vol. 18, no. 22, pp. 3553–3567, 2008. [Online]. Available: http://dx.doi.org/10.1002/adfm.200800541

[5] C. Li, E. T. Thostenson, and T.-W. Chou, "Sensors and actuators based on carbon nanotubes and their composites: A review," *Composites Science and Technology*, vol. 68, no. 6, pp. 1227 – 1249, 2008. [Online]. Available: http://www.sciencedirect.com/science/article/pii/S0266353808000171

[6] A. Tsioliaridou, C. Liaskos, E. Dedu, and S. Ioannidis, "Stateless linear-path routing for 3d nanonetworks," in *Proceedings of the 3rd ACM International Conference on Nanoscale Computing and Communication*. ACM, 2016, p. 28.

[7] L. Ferranti and F. Cuomo, "Nano-wireless communications for micrororobotics: An algorithm to connect networks of microrobots," *Nano Communication Networks*, 2017.

[8] E. Zarepour, M. Hassan, C. T. Chou, and M. E. Warkiani, "Characterizing terahertz channels for monitoring human lungs with wireless nanosensor networks," *Nano Communication Networks*, vol. 9, pp. 43–57, 2016.

[9] I. F. Akyildiz, J. M. Jornet, and C. Han, "Terahertz band: Next frontier for wireless communications," *Physical Communication*, vol. 12, pp. 16–32, 2014.

[10] L. Vangelista, A. Zanella, and M. Zorzi, "Long-range IoT technologies: The dawn of LoRa™," in *Future Access Enablers of Ubiquitous and Intelligent Infrastructures*. Springer, 2015, pp. 51–58.

[11] R. Ratasuk, N. Mangalvedhe, A. Ghosh, and B. Vejlgaard, "Narrowband lte-m system for m2m communication," in *Vehicular Technology Conference (VTC Fall), 2014 IEEE 80th.* IEEE, 2014, pp. 1–5.

[12] R. Ratasuk, B. Vejlgaard, N. Mangalvedhe, and A. Ghosh, "NB-IoT system for M2M communication," in *Wireless Communications and Networking Conference (WCNC)*. IEEE, 2016, pp. 1–5.

[13] D. C. Harrison, W. K. Seah, and R. Rayudu, "Rare event detection and propagation in wireless sensor networks," *ACM Computing Surveys (CSUR)*, vol. 48, no. 4, p. 58, 2016.

[14] C. Bisdikian, L. M. Kaplan, and M. B. Srivastava, "On the quality and value of information in sensor networks," *ACM Transactions on Sensor Networks (TOSN)*, vol. 9, no. 4, p. 48, 2013.

[15] J. Jornet and I. Akyildiz, "Femtosecond-long pulse-based modulation for terahertz band communication in nanonetworks," *IEEE Transactions on Communications*, vol. 62, no. 5, pp. 1742–1754, May 2014.

[16] P. Boronin, V. Petrov, D. Moltchanov, Y. Koucheryavy, and J. M. Jornet, "Capacity and throughput analysis of nanoscale machine communication through transparency windows in the terahertz band," *Nano Communication Networks*, vol. 5, no. 3, pp. 72–82, 2014.

[17] P. Wang, J. M. Jornet, M. A. Malik, N. Akkari, and I. F. Akyildiz, "Energy and spectrum-aware MAC protocol for perpetual wireless nanosensor networks in the Terahertz Band," *Ad Hoc Networks*, vol. 11, no. 8, pp. 2541–2555, 2013.

[18] J. M. Jornet, "Low-weight error-prevention codes for electromagnetic nanonetworks in the terahertz band," *Nano Communication Networks*, vol. 5, no. 1–2, pp. 35 – 44, 2014.

[19] T. A. Alsbou, M. Hammoudeh, Z. Bandar, and A. Nisbet, "An overview and classification of approaches to information extraction in wireless sensor networks," in *Proceedings of the 5th International Conference on Sensor Technologies and Applications (SENSORCOMM'11)*, 2011, p. 255.

[20] M. Pierobon, J. M. Jornet, N. Akkari, S. Almasri, and I. F. Akyildiz, "A routing framework for energy harvesting wireless nanosensor networks in the Terahertz Band," *Wireless Networks*, vol. 20, no. 5, pp. 1169–1183, 2014.

[21] H. Yu, B. Ng, and W. K. G. Seah, "On-demand efficient polling for nanonetworks under dynamic IoT backhaul network conditions," in *2016 IEEE 35th International Performance Computing and Communications Conference (IPCCC)*, Dec 2016, pp. 1–8.

[22] H. Yu, B. Ng, and W. K. G. Seah, "TTL-based Efficient Forwarding for the Backhaul tier in Nanonetworks," in *Proceedings of the 14th IEEE Annual Consumer Communications & Networking Conference (CCNC)*, Las Vegas, NV, USA, 8-11 Jan 2016.

[23] Z. S. H. Guo and J. M. Jornet, "A Cooperative Raman Spectrum Reconstruction Platform for Real-time In-vivo Nano-biosensing," in *Proc. of the INFOCOM Workshop on Wireless Communications and Networking in Extreme Environments (WCNEE)*, Atlanta, GA, USA, May 2017, pp. 1–6.

[24] S. D'Oro, L. Galluccio, G. Morabito, and S. Palazzo, "A timing channel-based MAC protocol for energy-efficient nanonetworks," *Nano Communication Networks*, vol. 6, no. 2, pp. 39–50, 2015.

[25] F. Peper, K. Leibnitz, J. n. Teramae, T. Shimokawa, and N. Wakamiya, "Low-complexity nanosensor networking through spike-encoded signaling," *IEEE Internet of Things Journal*, vol. 3, no. 1, pp. 49–58, Feb 2016.

[26] G. Piro, L. A. Grieco, G. Boggia, and P. Camarda, "Nano-sim: simulating electromagnetic-based nanonetworks in the network simulator 3," in *Proc. of the 6th International ICST Conference on Simulation Tools and Techniques*, Cannes, French Riviera, 5-7 March 2013, pp. 203–210.

[27] Y. L. Babikov, I. E. Gordon, S. N. Mikhailenko, L. S. Rothman, and S. A. Tashkun, "HITRAN on the Web – a new tool for HITRAN spectroscopic data manipulation," in *Proceedings of the 12th International HITRAN Conference*, 29-31 August 2012.

[28] Q. H. Abbasi, K. Yang, N. Chopra, J. M. Jornet, N. A. Abuali, K. A. Qaraqe, and A. Alomainy, "Nano-communication for biomedical applications: A review on the state-of-the-art from physical layers to novel networking concepts," *IEEE Access*, vol. 4, pp. 3920–3935, 2016.